

## Correlating deformation and metamorphism around orogenic arcs

T.H. BELL AND V.M. MARES

School of Earth Sciences, James Cook University, Townsville, Queensland 4811, Australia

### ABSTRACT

The timing of metamorphism and the  $P$ - $T$ - $t$  path the rocks have undergone commonly varies around orogenic arcs, hindering correlation along orogens. Isotopic dating enables broad correlations to be made, but detailed correlations can be difficult using this approach where several phases of metamorphism are present. This is compounded by the large size of oroclinal arcs, which hinders correlation of deformation and metamorphism using a succession of structures and associated metamorphism. However, foliation inflexion-intersection axes (FIAs) preserved in porphyroblasts provide a tool for correlation around oroclinal arcs. Consistent successions of FIAs that remain constantly oriented around folds and across large tracts of multiply ductilely deformed country rock allow correlation of periods of metamorphism taking place during the one direction of horizontal bulk shortening, rather than correlation of inferred growth events. Consequently, rocks that have undergone different  $P$ - $T$ - $t$  paths can be correlated.

Measurement of FIAs around the spectacular Kimberley Arc in northwest Australia reveals that the first-formed set maintain a consistent average trend of  $127^\circ$  and a subhorizontal plunge. This FIA trend is parallel to the western arm of the arc, but lies at a very high angle to the eastern arm. Foliations preserved as inclusion trails in porphyroblasts are continuous with foliations in the matrix on the western arm, where the FIAs and structural grain are sub-parallel. However, inclusion trails in porphyroblasts defining FIAs with these same trends on the eastern arm are truncated by the matrix foliation. This indicates that foliations in the matrix on the eastern arm postdate all foliations in the matrix on the western arm. Two late sets of locally developed, small kinks of the matrix foliation on the western arm, which have axial planes parallel to foliations on the eastern arm, are weak expressions of the overprinting events that controlled the geometry of the latter arm.

A second group of FIAs has been found in some samples on the eastern arm that lie sub-parallel to the northeast trend of this arm. They are defined by inclusion trails that are continuous with the matrix foliation and that occur in the rims of porphyroblasts. Such porphyroblasts generally contain a core with inclusion trails defining the first-formed FIA that lies sub-parallel to the western arm. The inclusion trails in porphyroblast cores are truncated completely by those in the rims, in the same manner that those without this rim-set of inclusion trails are truncated by the matrix foliation. This second set of FIAs has not been found in any samples from the western arm.

FIAs thus provide a simple tool for correlating metamorphism around orogenic arcs. The porphyroblasts with consistently oriented FIAs around the arc can be readily correlated and grew during the same period of metamorphism that affected both arms. Those with northeast-trending FIA record a younger period of metamorphism that affected only the eastern arm. Indeed, until techniques and standards for dating porphyroblasts and their inclusions by both the microprobe and ion-microprobe improve, FIAs may provide the only quantitative tool that integrates metamorphic and structural phenomena and thus allows detailed correlation of these events along an orogen.

### INTRODUCTION

Most orogens are arcuate on a large scale. Some of these arcs were formed by bending of the mountain belt, subsequent to its formation, producing structures called oroclinal arcs (Carey 1955); others may have formed with a bent shape (Marshak 1988). Some orogens are strikingly arcuate, such as the Western Arc of the Alps (Platt et al. 1989) and the Nackara Arc of the Adelaide Fold Belt (Bell 1978). Other orogens are less obviously arcuate but change orientation relatively regularly along

their whole length (e.g., the multiple arcs along the Appalachians). Correlating deformation and metamorphism around such large-scale arcs is difficult (without isotopic dates), especially since the succession or orientation of pervasive or overprinting structures in the rock matrix may not be useful as a guide; such structures may be reoriented around the arc, or not present on one arm of the arc. The large scale of arc development makes correlation of structural and metamorphic successions arduous and introduces a degree of uncertainty. Isotopic dating generally only allows correlation of the broad timing of orogenesis (e.g., Acadian vs. Taconic or Alleghanian along the Appalachians), rather than a fine-scale correlation of phases

---

\*E-mail: tim.bell@jcu.edu.au

of metamorphism and deformation events and associated bulk movement directions, because it tends to reflect the peak of metamorphism or later phases of retrogression. A succession of mineral growth phases prior to peak metamorphism, such as those that have been recorded in the Vermont Appalachians (Bell et al. 1998), are very difficult to date isotopically.

Detailed work in the Appalachians using a succession of foliation inflexion or intersection axes (FIA) preserved by inclusion trails in porphyroblasts has revealed that such structures can remain unaffected by multiple episodes of subsequent folding. This allowed the correlation of multiple porphyroblast growth episodes about successive FIA trends, and hence equivalent periods of metamorphism, across macroscopic fold limbs (Bell and Hickey 1997; Bell et al. 1997; Hickey and Bell 1999) and over large tracts of multiply deformed and metamorphosed rocks (Bell et al. 1998). It suggests that FIAs might enable correlation of periods of metamorphism, through correlating periods of porphyroblast growth, around oroclinal arcs. Consequently, we have conducted a study to test this around one of the most spectacular arcuate-shaped orogens in the world, the Kimberley Arc (Fig. 1).

### THE KIMBERLEY ARC

The Kimberley region of far-north Western Australia (Fig. 1) is bordered by a Precambrian orogen that curves to form the Kimberley Arc. The materials within the orogen consist of turbiditic metasedimentary rocks, felsic volcanic rocks, granitoid plutons, gabbro bodies, and dolerite (diabase) dikes (Dow and Gemuts 1969; Gemuts 1971; Derrick and Playford 1973; Plumb and Gemuts 1976; Griffin et al. 1992). The deformation and metamorphism on both sides, or arms, of the arc are known to be broadly coeval, spanning the period from 1880 to 1820 Ma (Page 1988; Page and Sun 1994; Page et al. 1995a, 1995b).

#### The western arm

Portions of the west-northwest-trending western arm of the Kimberley Arc (Fig. 1; called the King Leopold orogen) have been affected by at least 6 stages or phases of ductile deformation. Metamorphism accompanied deformation and produced widespread garnet-, kyanite-, sillimanite-, and staurolite-bearing assemblages in metasedimentary rocks called the Marboo Formation (Mares 1996). Figure 2 shows three areas (boxes a, b, and c in Fig. 1) that have been mapped in detail. A schistosity,  $S_1$ , is everywhere parallel to compositional layering,  $S_0$ .  $S_2$  is only locally preserved in the more psammitic layers as a very fine schistosity, and lies sub-parallel to  $S_{0,1}$  (equal-area nets in Fig. 2c).  $S_3$  is a well-developed, differentiated crenulation cleavage at stage 4 to 5 (Bell and Rubenach 1983) and generally lies at a low angle to  $S_{0,1}$  (maps and stereographic nets in Figs. 2a–c), except in the hinges of macroscopic  $F_3^0$  folds (Figs. 2a and 2b).  $S_4$  is a well-developed crenulation cleavage in pelitic layers, and tends to lie oblique to the earlier structures.  $S_5$  forms the axial plane of small, locally developed kinks and lies at a high angle to the structural grain (stereographic nets in Figs. 2a, 2b, and 2c).  $S_6$ , where present, occurs as the sub-horizontal axial planes of very locally developed open folds (Fig. 2c). Thus  $D_1$ ,  $D_2$ ,  $D_3$ , and, to some extent,  $D_4$  structures are colinear and trend west-northwest, approximately parallel

to this portion of the arc. The younger structures tend to lie at a high angle to the west-northwest structural grain.

The Hawkstone Creek area (area b in Fig. 1; Fig. 2b) contains two distinct mineral assemblages. The psammitic portion SW of the kyanite isograd contains biotite-kyanite-quartz. The pelitic portion northeast of this isograd contains assemblages of garnet-staurolite-biotite-quartz with rare andalusite and sillimanite. The Napier area (area a in Fig. 1; Fig. 2a) contains kyanite (replacing andalusite)-sillimanite-biotite-muscovite-quartz and garnet-staurolite-biotite-muscovite-quartz assemblages. The Windjana area (area c in Fig. 1; Fig. 2c) contains garnet-biotite-quartz-muscovite assemblages. The Sparke Range area (area e in Fig. 1) contains an assemblage of andalusite (variably retrogressed to sericite)-biotite-muscovite-quartz.

#### The eastern arm

Portions of the north-northeast-trending eastern arm of the Kimberley Arc (Fig. 1; called the Halls Creek orogen) also have been affected by at least six stages of ductile deformation accompanied by metamorphism that produced rocks ranging from sub-greenschist to granulite facies (Allen 1985, 1986; Mares 1996). Figure 3 shows a detailed map of the Black Rock Antiform (in Fig. 1, box d). Bedding is evident in this region as coarse-scale compositional layering. Foliations that predate the earliest ones present in the matrix are preserved as inclusion

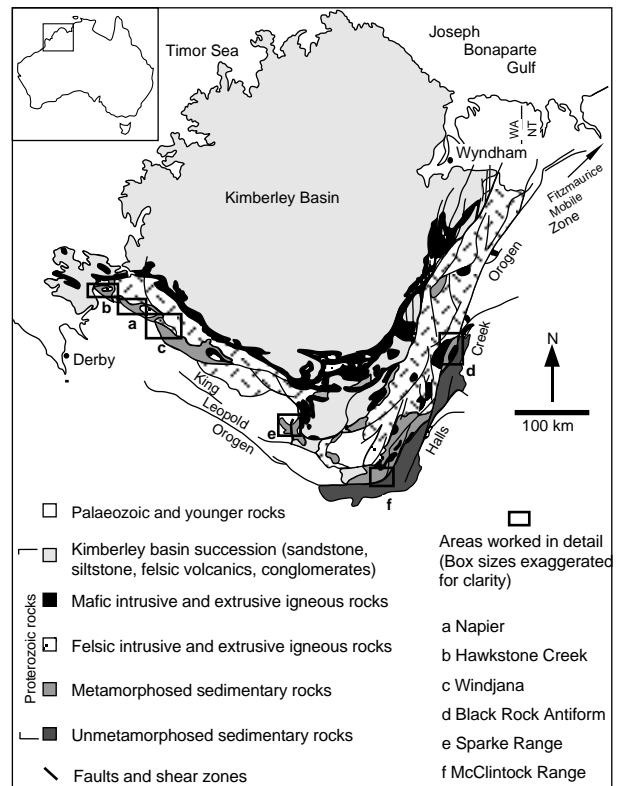


**FIGURE 1.** Location and geologic map of the Kimberley showing the arc. Location of areas where detailed mapping was done as well as areas where samples were taken are indicated with boxes marked a, b, c, d, e, and f.

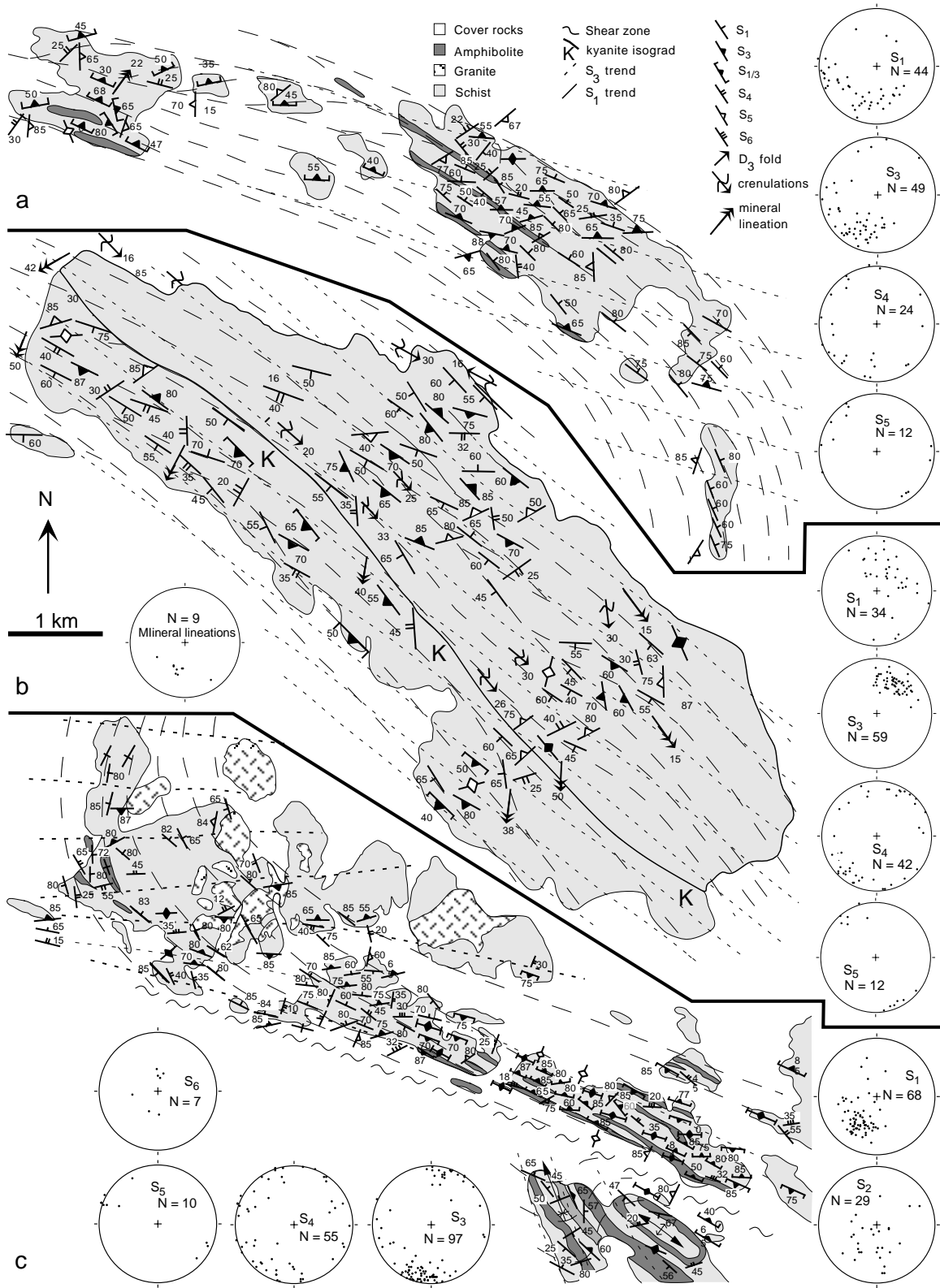


FIGURE 2. Geological maps of the Napier, Hawkstone Creek, and Windjana areas (areas labeled boxes a, b, and c in Fig. 1).

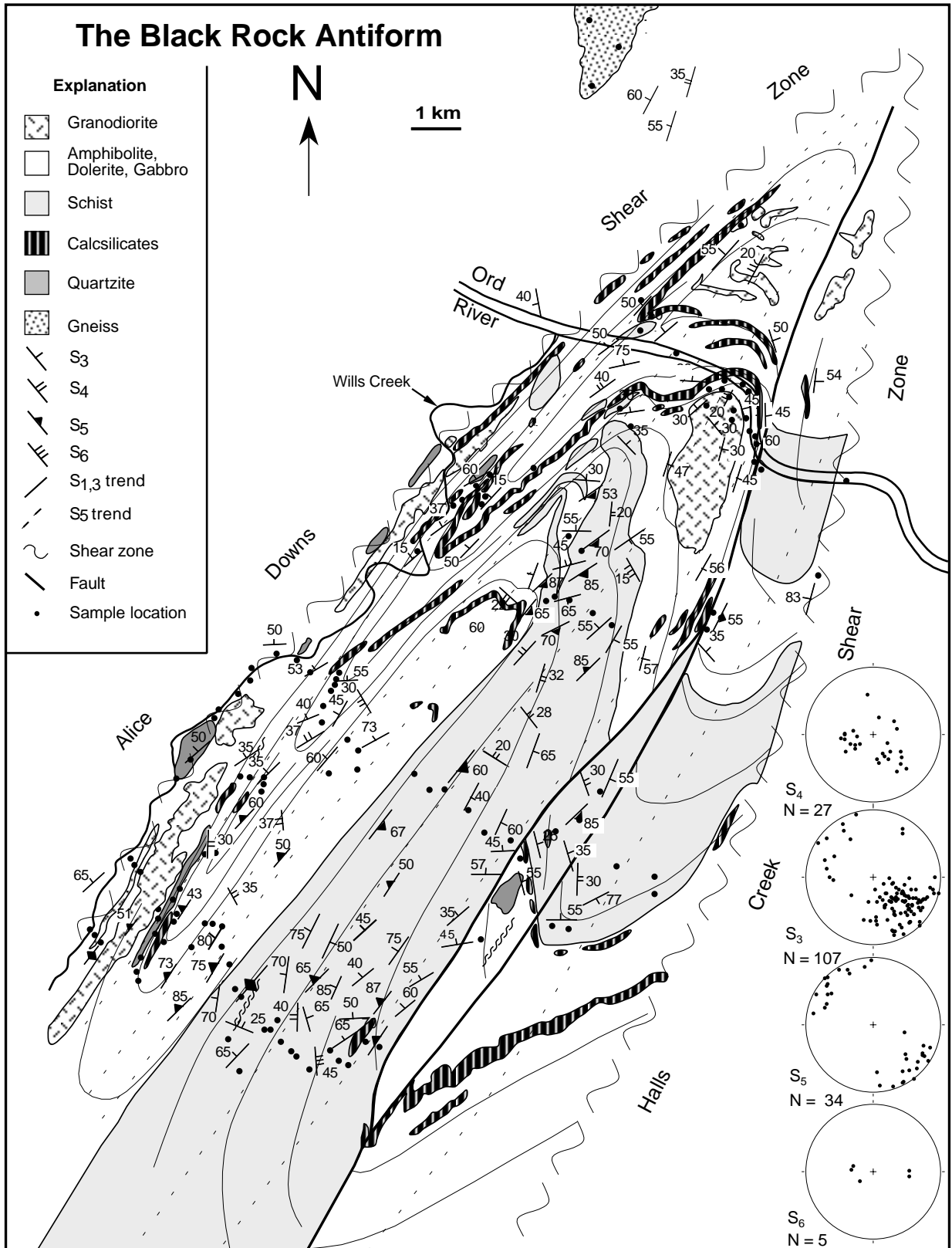


FIGURE 3. Geological map of the Black Rock Anticline (area labeled box d in Fig. 1).

trails in porphyroblasts, but are truncated by the younger matrix foliations (see below). The first foliation seen in the matrix is at least the third foliation, but is called  $S_{1,3}$  to show that earlier foliations (preserved in porphyroblasts) predate it, but now lie parallel to  $S_3$ . An isoclinal  $D_3$  fold (left side of Fig. 3) is refolded by a macroscopic isoclinal  $D_5$  fold, called the Black Rock Antiform (center of Fig. 3), such that  $S_{1,3}$  and  $S_5$  are sub-parallel except in the  $D_5$  fold hinge.  $S_4$  occurs as shallowly dipping axial planes of recumbent  $D_4$  folds.  $S_5$  strikes parallel to  $S_4$ , and  $S_6$  forms the subhorizontal axial planes to weakly developed open folds.  $D_3$ , and younger folds and foliations, are effectively colinear in that their successive intersections trend northeast parallel to this portion of the arc.

The Black Rock anticline (box d in Fig. 1; Fig. 3) contains assemblages of biotite-quartz-muscovite-sillimanite (fibrous) and rare garnet in the west and garnet-biotite-muscovite-quartz in the east. The McClintock Range area (box f in Fig. 1) contains andalusite-biotite-muscovite-garnet-quartz assemblages with the andalusite commonly retrogressed to sericite.

### Both arms

Both arms of the arc preserve similar ages of granitoid emplacement (1865–1850 Ma in the west vs. 1860–1855 Ma in the east, Tyler et al. 1994). Both arms also preserve long histories of multiple deformation and similar isotopic ages for peak metamorphism determined using U-Pb ages from anatectic rock associated with migmatitic gneisses (1855 ± 5 Ma vs. 1854 ± 5 Ma; Tyler et al. 1994; Page et al. 1995b). However, the rocks on

the eastern arm also show a younger period of tonalite emplacement (1830–1820 Ma) and regional metamorphism (1830 ± 3 Ma, from zircon crystallized in leucosome bands in garnet-bearing paramigmatite) that is not present in the western arm (Page et al. 1995b; Tyler and Page 1996). With this age control, precise correlation of specific structures and associated metamorphism should be possible along the length of the arc because it is such a distinctive and continuous orogen, isolated from all other orogens in the region. However, the radically different orientations and large scale of each arm, and the younger deformation and metamorphism that dramatically affected the eastern arm, but only slightly affected the western arm, make this a very difficult task. This difficulty is magnified by the fact that inclusion trails in the great majority of garnet porphyroblasts in the eastern arm are truncated by the matrix foliations, destroying all normal timing criteria that might allow direct correlation of mineral growth periods (see below).

### INCLUSION TRAILS IN GARNET PORPHYROBLASTS

Garnet porphyroblasts in rocks from the western arm commonly contain inclusion trails that are continuous with matrix foliations, as shown in Figure 4. Many garnet porphyroblasts in rocks from the eastern arm contain inclusion trails that are either completely truncated by the matrix foliation (Fig. 5), connected to it by trails in a narrow rim that truncate the trails in the core (Fig. 6), or show a dramatic switch in asymmetry from core to rim (Fig. 7). Consequently, the timing of metamorphism relative to matrix microstructures, and hence defor-

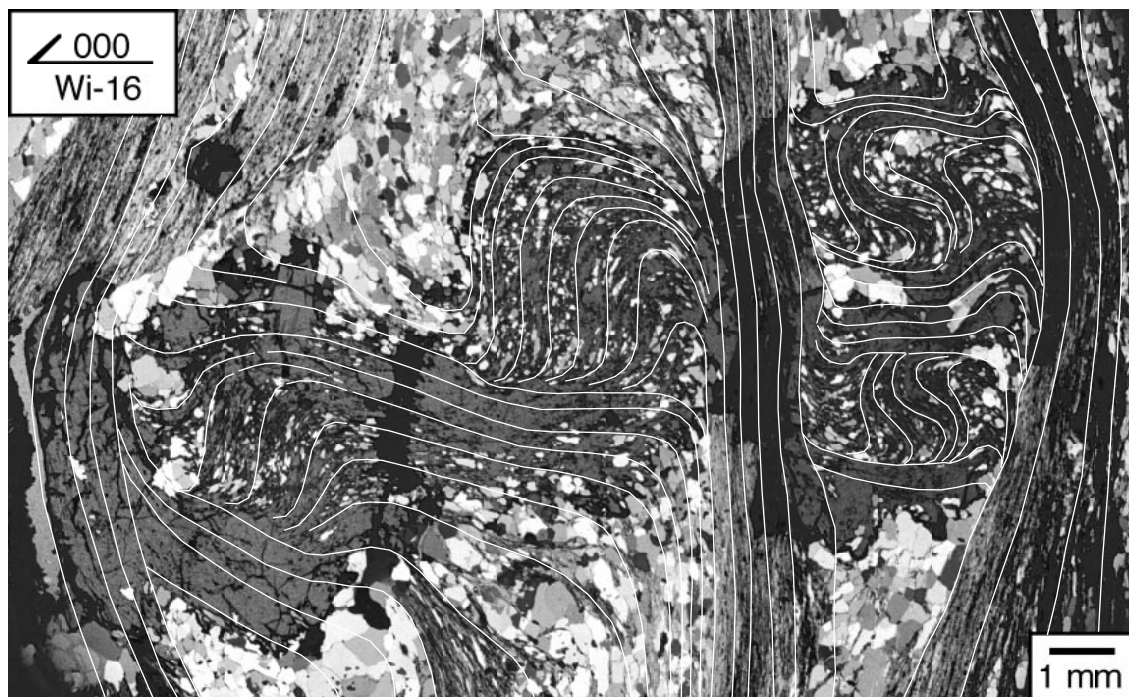


**FIGURE 4.** Photomicrograph showing continuity of inclusion trails within garnet porphyroblasts and the matrix foliation in western arm of the Kimberley Arc where the FIA average 127°. A distinctive sub-horizontal zone of differentiated crenulation cleavage, preserved in the rim of each porphyroblast, is in turn overprinted by a vertical differentiated crenulation cleavage. Partially crossed polars. Vertical section with strike shown by horizontal, single-barbed arrow. (Sample Wi16 located in area c in Fig. 10.)

mation events, could not be determined for the bulk of garnet porphyroblasts on the eastern arm. This made correlation of pre-matrix phases of metamorphism on this arm with that in the western arm impossible using a classic approach. Some samples were found in which relatively simple inclusion trail geometries are continuous with the matrix foliation across the whole porphyroblast (Fig. 8).

FIA measured from inclusion trails in the porphyroblasts record the orientation of the overprint of successive foliations on one another, providing quantitative orientation data that allow the separation of periods of porphyroblast growth indistinguishable by other means (e.g., Bell et al. 1995, 1997, 1998; Bell and Hickey 1997; Chen, A. unpublished manuscript 1999; Kim, H.S. unpublished manuscript 1999). From 58 oriented samples collected around the Kimberley Arc, 64 FIA were determined (Table 1). The bulk of these samples came from the areas mapped in detail (Figs. 2 and 3). However, extra samples were collected from two other locations (Fig. 1, boxes e and f) to test for variation in FIA trends in other portions of the arc. From each of the samples we cut numerous (up to 23) spatially



**FIGURE 5.** Garnet porphyroblast with inclusion trails truncated completely by the matrix foliation. The foliation in the matrix, which truncates the inclusion trails in the porphyroblast, has been partially sericitized post foliation development as the tiny muscovite grains have random orientations. This has not affected the inclusion trail geometry or the matrix foliation geometry. Plane polarized light. FIA trends  $135^\circ$ . Vertical section with strike shown by horizontal, single-barbed arrow. (Sample H301 located in Fig. 12.)

oriented vertical thin sections with different strikes (Table 1). The asymmetry of inclusion trail curvature (clockwise or anticlockwise sense of progressive curvature outward from porphyroblast core to rim) within porphyroblasts intersected by each thin section was used to determine the orientation of the FIA preserved within them (Fig. 9; Bell et al. 1995). The sections across which the asymmetry flips when viewed in one

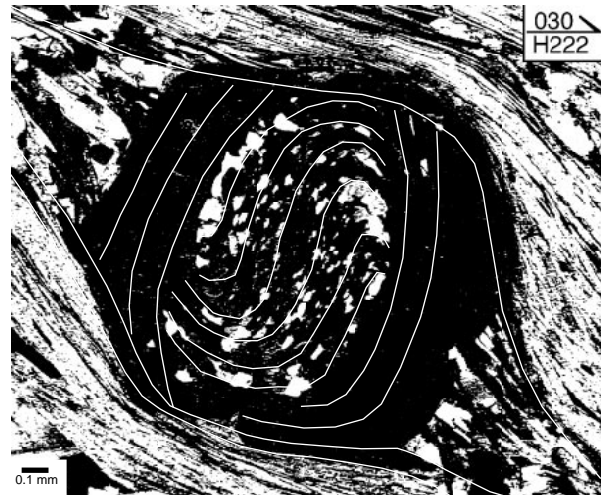


**FIGURE 6.** Garnet porphyroblast with inclusion trails in a narrow rim that connect to the matrix foliation, but which truncate the trails in the core. The FIA in the core is oriented  $115^\circ$ . The inclusion trails in the rim are continuous with those in the matrix and define a FIA trending at  $35^\circ$ . Vertical section with strike shown by horizontal, single-barbed arrow. (Sample H222 located in Fig. 12.)

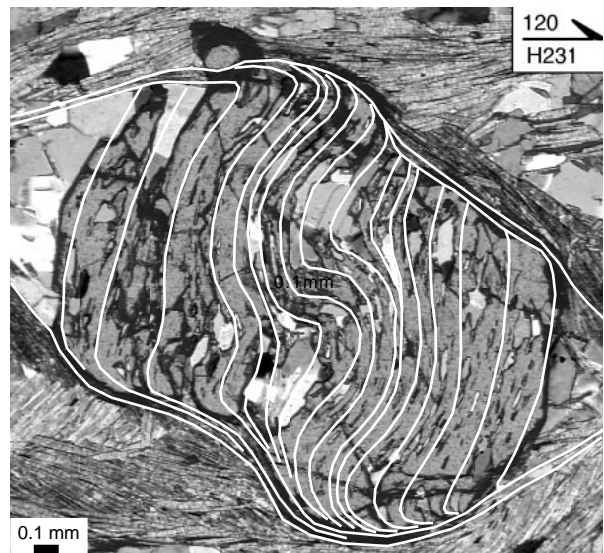


**FIGURE 7.** Garnet porphyroblast with inclusion trails showing a dramatic switch in asymmetry from core to rim. The FIA for the core is  $115^\circ$  whereas that for the rim is  $35^\circ$ . The trails on the rim are continuous with the matrix. Partially crossed polars. Vertical section with strike shown by horizontal, single-barbed arrow. (Sample H231 located in Fig. 12.)

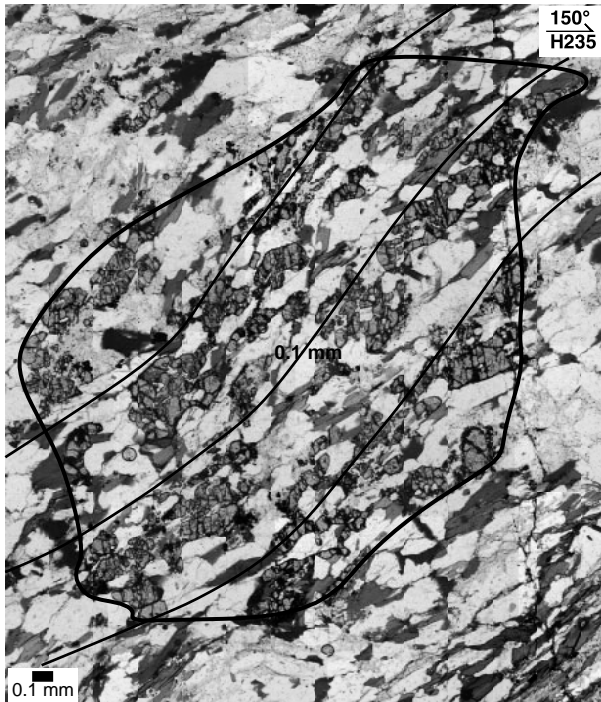


**FIGURE 8.** Poikiloblastic garnet porphyroblast with inclusion trails continuous with the matrix foliation. Plane polarized light. Vertical section with strike shown by horizontal, single-barbed arrow (Sample H235 located in Fig. 12).

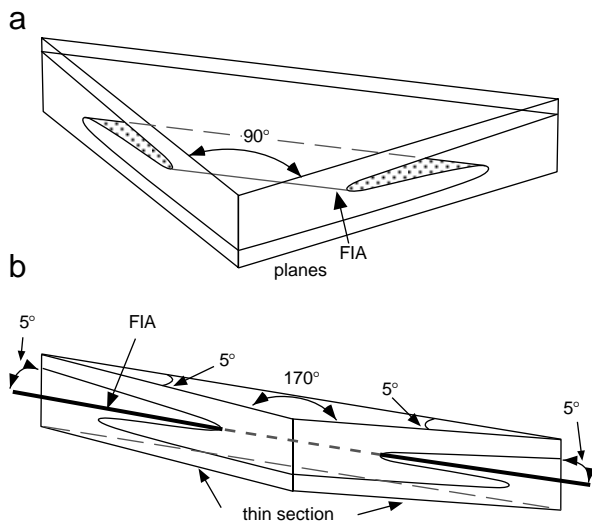


**FIGURE 9.** (a) 3-D sketch of an asymmetric  $S_1$  cut by two vertical planes lying to either side of the axis. When viewed from the same direction the asymmetry flips across the axis. (b) The trend of the axis shown in "a" can be defined by finding two differently striking vertical thin sections between which the  $S_1$  asymmetry flips when viewed in the same direction.

direction define the bounds of the possible FIA trend (Fig. 9; the technique for measuring a sample with more than one FIA is described by Bell et al. 1998). For almost all the samples in this study, the flip in asymmetry was narrowed down to two sections  $10^\circ$  apart and the FIA trend was assumed to lie midway between the two sections defining the change. In a few samples, one thin section was found to contain porphyroblasts with both asymmetries, whereas those  $10^\circ$  to either side had opposite asymmetries. In these cases the FIA trend was taken to lie in the thin section plane containing both asymmetries. If the FIA changes orientation from the core to the rim of the porphyroblast, its trend in both positions can be determined (Bell et al. 1998). Changes in FIA trend from core to rim have particular significance for the correlation of porphyroblast growth around the Kimberley Arc. The results obtained have allowed us to distinguish two different phases of garnet growth on the eastern arm (see below), and to determine their relative timing.

The same geometric principle allows the plunge of the FIA to be determined by cutting a series of differently dipping sections striking perpendicular to the FIA trend and finding the two sections between which the asymmetry of  $S_1$  curvature flips when viewed looking down from above (Fig. 7 in Bell et al. 1995). FIA plunges have been determined for 7 samples across the arc using this technique (Table 1).

The total accumulated error in determining the trend or plunge of an FIA using the method described above is estimated as  $\pm 8^\circ$  (Bell and Hickey 1997).<sup>1</sup> In samples where more than one FIA was determined, possible errors in their relative trends are only a function of the last two stages of sample preparation and they should have a relative precision of  $\pm 4^\circ$ .

#### FIA TRENDS ON THE WESTERN ARM OF THE ARC

The FIA from the areas that were mapped in detail on the western arm of the Kimberley Arc (Fig. 2) trend west-northwest to east-southeast, parallel to the axial planes of the macroscopic folds and the trend of the orogen (Fig. 10). The FIA trend throughout areas a and c is remarkably consistent (averaging  $127^\circ$ ), and is independent of location on macroscopic folds (cf. Bell and Hickey 1997; Bell et al. 1997, 1998; Hickey and Bell 1999; A. Chen, unpublished manuscript 1999; H.S. Kim, unpublished manuscript 1999). The three areas shown in Figure 10 span a distance of  $>100$  km along the orogen (areas a, b, and c in Fig. 1) and yet have similar FIA trends. This consistency in FIAs becomes more remarkable when FIA data from area e in Figure 1 are examined. Although this area is still located on the western arm of the Kimberley Arc, it lies 200

<sup>1</sup>This value was arrived at in the following manner: the precision of the compass is  $\pm 1^\circ$ , hence this is the error involved in measuring and marking the orientation on the sample in field; repositioning the compass relative to orientation mark on rock face in laboratory,  $\pm 2^\circ$ ; precision error of compass used to reorient sample in laboratory,  $\pm 1^\circ$ ; error in cutting sample into horizontal slabs and marking north on them (for plunge determinations vertical slabs were prepared and horizontal was marked on them),  $\pm 2^\circ$ ; error in marking on and cutting thin section blocks from these slabs  $\pm 2^\circ$ . The errors are all random and all of the same order of magnitude.

**TABLE 1.** Sample numbers, FIA trends, and strike of thin sections

| Sample (FIA trend*)             | Strikes of vertical thin sections used in degrees (number of sections made)  |
|---------------------------------|--|
| <b>Napier (4)</b>               |  |
| WG-277A (135)                   | 0, 30, 60, 90, 120, 130, 140, 150  |
| WG-293 (15→135)*                | 0, 10, 20, 30, 40, 50, 60, 70, 80, 90, 100, 110, 120, 130, 140, 150, 160, 170. Strikes 225, dips 0, 10, 20SE, 10, 20NW |
| WG-294 (135)                    | 0, 30, 60, 90, 120(2), 130, 140(2), 150  |
| WG-299 (125)                    | 0, 30, 60, 90, 120, 130, 140, 150(2), 160(2), 170(3)   |
| <b>Hawkstone(1)</b>             |  |
| V-251B (135)                    | 0, 30, 60, 90, 120, 130, 140, 150  |
| <b>Windjana (33)</b>            |  |
| Wi-3A (115)                     | 0, 30(2), 60, 90(5), 100, 110, 120(4), 150(4)  |
| Wi-6 (145)                      | 0(3), 30(3), 60(3), 90(2), 120(4), 130, 140, 150(6)  |
| Wi-8 (115)                      | 0, 30, 60, 90, 100, 110, 120, 150  |
| Wi-9B (135)                     | 0, 30, 60, 90, 120, 130, 140, 150  |
| Wi-16 (135)                     | 0, 30, 60, 90, 120, 130(2), 140, 150, 160(5)   |
| Wi-17 (135)                     | 0, 30, 60, 90, 120, 150  |
| Wi-18 (135)                     | 0, 30, 60(2), 90, 120(2), 150(2)   |
| Wi-21 (125)                     | 0, 30, 60, 90, 120, 130, 140, 150  |
| Wi-24C (135)                    | 0, 30, 60, 90, 120, 130, 140, 150  |
| Wi-27 (125)                     | 0, 30, 60, 90(2), 120(2), 130, 140, 150  |
| Wi-28 (120)                     | 0, 30(3), 60, 90, 120(2), 130(2), 140(2), 150, 160, 170(2)   |
| Wi-29 (120)                     | 0(3), 20(2), 30(3), 60(2), 70, 90(4), 120(4), 130(2), 140(2), 150(4), 160, 170(3)                                      |
| Wi-32 (125)                     | 0, 30, 60, 90, 120, 130, 140, 150  |
| Wi-42 (125)                     | 0, 30, 60, 90(3), 120, 130, 140, 150   |
| Wi-44 (125)                     | 0, 30, 60, 90, 120, 130, 140, 150  |
| Wi-45 (115)                     | 0, 30, 60, 90, 100, 110, 120, 150  |
| Wi-50 (115)                     | 0, 30, 60(4), 90(6), 100, 110, 120(3), 150(2)  |
| Wi-101 (145)                    | 0, 30, 60, 90, 120, 130, 140, 150  |
| Wi-220 (145)                    | 0, 30, 60, 90, 120, 130, 140, 150  |
| Wi-221A (135)                   | 0, 30(2), 60, 90, 120, 130, 140, 150   |
| Wi-222 (105)                    | 0, 30, 60, 90, 100, 110, 120, 150  |
| Wi-232 (140)                    | 0, 30, 60, 90, 120, 130, 140, 150  |
| Wi-241B (125)                   | 0, 30(2), 60, 90, 120, 130, 140, 150   |
| Wi-244 (115)                    | 0, 30, 60, 90, 100, 110, 120, 150  |
| Wi-249 (120)                    | 0, 30, 60, 90, 120, 150  |
| Wi-252 (135)                    | 0, 30, 60, 90, 120, 150  |
| Wi-255B (125)                   | 0, 30, 60, 90, 120, 130, 140, 150  |
| Wi-257R (115)                   | 0, 30, 60, 90, 100, 110, 120, 150  |
| Wi-2111A (125)                  | 0, 30, 60, 90, 100, 110, 120, 130, 140, 150  |
| Wi-2112A (5→115)*               | 0, 30, 60, 90, 100, 110, 120, 130, 140, 150. Strikes 205, dips 0, 10, 20SE, 10, 20NW                                   |
| LR3 (105)                       | 0, 30, 60, 90, 100, 110, 120, 150  |
| LR4 (135)                       | 0, 30, 60, 90, 120, 130, 140, 150  |
| <b>Black Rock Antiform (19)</b> |  |
| H-104 (135)                     | 0, 30, 60, 90, 120, 130, 140, 150  |
| H-105B (135-c, 25-r)            | 0, 20, 30, 60, 90, 120, 130, 140, 150  |
| H-111 (120-c, 30-r)             | 0, 30, 60(2), 120, 130, 140, 150(2), 160   |
| H-115 (135)                     | 0, 30, 60, 90, 120, 130, 140, 150, 30(hz)  |
| H-209 (125)                     | 0, 30, 60, 90, 120, 130, 140, 150  |
| H-221D (5→135)*                 | 0, 30, 60(2), 130, 140, 150. Strikes 225, dips 0, 10, 20SE, 10, 20NW   |
| H-222 (0→115)*                  | 0, 30, 60, 90(2), 100, 110, 120, 150. Strikes 205, dips 0, 10, 20SE & 10, 20NW   |
| H-227 (25→145-c, 45-r)*         | 0, 30, 40(2), 50(2), 60, 90, 120, 140, 150, 160. Strikes 235, dips 0, 10, 20SE & 10, 20, 30, 40NW                      |
| H-231 (115-c, 45-r)             | 0, 30, 40, 90, 100, 110, 120, 130, 140, 150  |
| H-235 (45)                      | 0, 30, 40, 50, 60, 90, 120, 150  |
| H-266 (130)                     | 0, 30, 60, 90, 120, 140, 150, 160  |
| H-267 105, (0→25)*              | 0, 10, 20, 30, 60, 90, 120, 150. Strikes 115, dips 0, 10, 20NE & 10, 20SW  |
| H-301 (135)                     | 0, 30(2), 60, 90, 120, 130, 140, 150   |
| H-303 (125)                     | 0, 30, 60, 90, 120, 130, 140, 150, 30(hz)  |
| H-304 (135)                     | 0, 30, 60, 90, 120, 130, 140, 50   |
| <b>Sparke (2)</b>               |  |
| G-3 (120)                       | 0, 30, 60, 90, 120, 150  |
| G-4 (135)                       | 0, 30, 60, 90, 120, 150  |
| <b>McClintock (5)</b>           |  |
| L1A (130-a, 20-g)               | 0, 10, 20, 30, 60, 90, 120, 130, 140, 150  |
| L2B (15→135-a, 45-g)*           | 0, 30(2), 40, 50, 60, 70(2), 80(2), 90(3), 120, 130, 140, 150. Strikes 225, dips 0, 10, 20SE, 10, 20NW                 |
| L1C2 (135)                      | 0, 30, 60, 90(2), 120(2), 130, 140, 150(2)   |

*Notes:* Sample numbers, FIA trends shown in brackets after sample number; and thin section strikes of the vertical thin sections cut to determine these trends (numbers in brackets refer to number of sections cut where more than one) arranged in terms of the area locations (number after area name refers to total FIA determinations from that region) shown in Figure 1. For area 5 (McClintock Range) a = andalusite, g = garnet. For area 6 (Black Rock Antiform) c = core FIA, r = rim FIA. The sample numbers, plunge and plunge direction (in brackets) and dip and dip directions of thin sections used to determine these plunges are shown for several samples spanning the 6 areas in Figure 1. The 105° FIA trend for the core of Sample H267 was only determined within a total range of 30°.

\* Plunge and trend of FIA is given—strike and dip of sections used to determine plunge are also given.

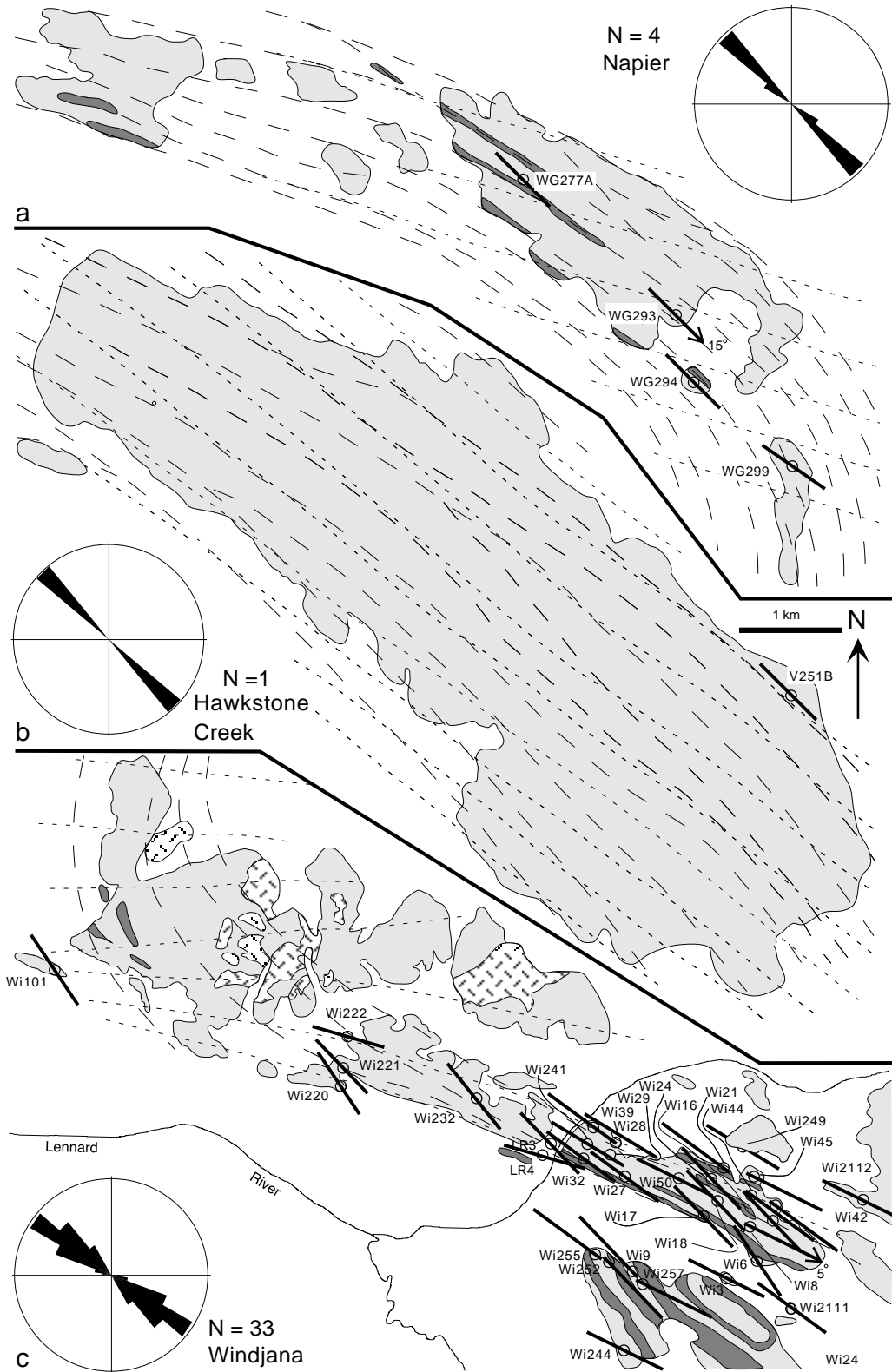


FIGURE 10. Maps from Figure 2 showing the locations and trends of the FIA in garnet porphyroblasts determined for the samples shown. Two FIA for which the plunge was determined are shown for areas a and c.

km further east and the trend of the orogen has swung clockwise (see below) through more than  $45^\circ$  to almost due South; yet the FIA trends here remain the same as those in areas a, b, and c in Figure 1. That is, the FIA trends on the western arm of the Kimberley Arc, although sub-parallel to the bulk of the trend of this arm, are independent of this trend (Fig. 11; see below).

#### FIA TRENDS ON THE EASTERN ARM OF THE ARC

Samples from the Black Rock Antiform on the eastern arm of the arc exhibit two modal peaks in FIA trend—a larger one at  $127^\circ$  and a smaller one at  $035^\circ$  (Fig. 12). Four samples from this area have differently trending FIAs in their core and rim. In all cases the core FIA has an east-southeast trend, whereas the rim FIA has a north-northeast to northeast trend (Table 1). This consistent relationship suggests that the set of southeast-

trending FIA predate the northeast-trending set. This timing is supported by the youngest subvertical structures in the western arm being aligned northeast ( $S_5$  in Figs. 2a–c), whereas the earlier ones are aligned northwest.

#### The older FIA set

The dominant older  $127^\circ$ -trending FIA set lies at a high angle to the structural trends in this region (compare Figs. 3 and 12). The foliations defining this FIA trend are always truncated, either by the matrix foliations or by foliations in the garnet rims that are continuous with the matrix. Consequently, this FIA trend predates  $S_5$ .

FIA were also determined in samples from McClintock Range, some 200 km to the south, which contain both andalusite and garnet porphyroblasts (Fig. 1, area f). This area lies on the

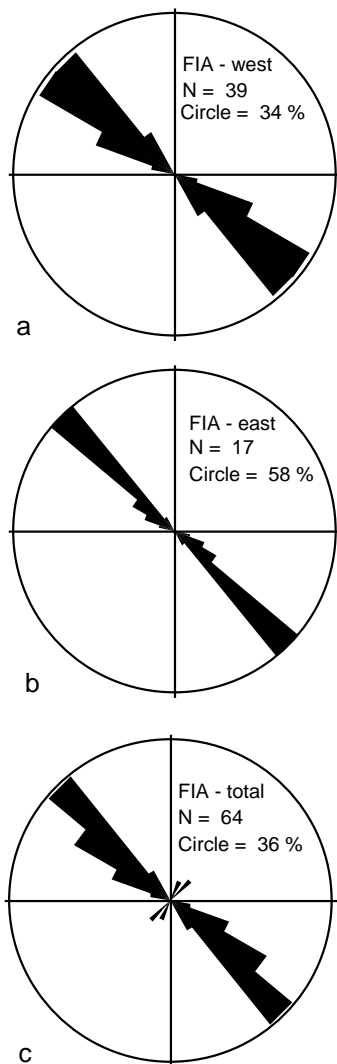


**FIGURE 11.** (a) Rose diagram of all FIAs from the western arm of the Arc. (b) Rose diagram of all northwest-southeast trending FIAs from the eastern arm of the Arc. (c) Rose diagram showing all FIAs from both arms of the Arc.

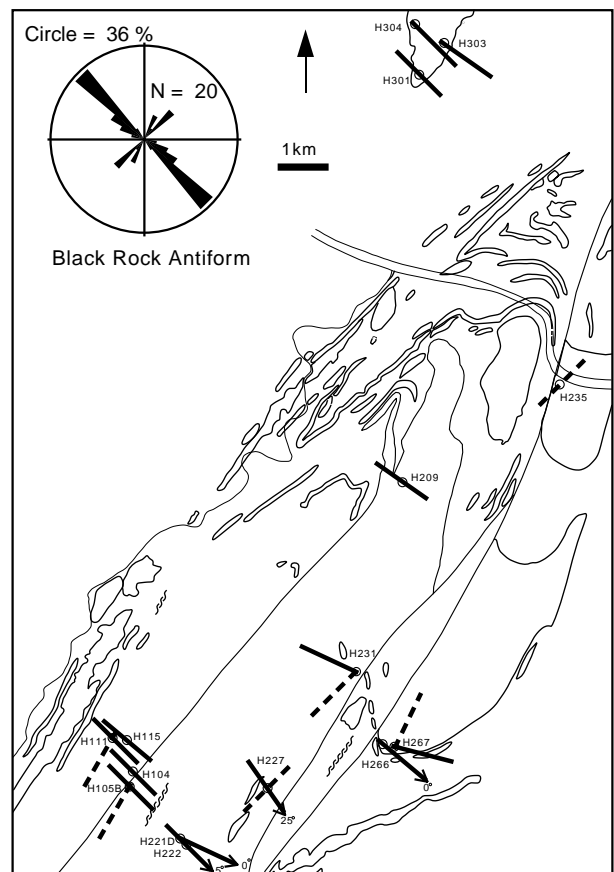


**FIGURE 12.** Map from Figure 3 showing the locations and trends of the FIA in garnet porphyroblasts determined for the samples shown. Of the 20 axes measured, 14 are oriented at a high angle to the regional structural trend. The 6 trending parallel to the regional structural trend appear to have formed after those at a high angle to it. Solid lines represent trends of core FIA where inclusion trails in garnet porphyroblasts are truncated by the matrix foliation or a foliation in the rim of the garnet that is continuous with the matrix foliation. Dashed lines represent trends of rim FIA where the foliation truncates that in the core and is continuous with that in the matrix. Four FIA for which the plunge was determined are also shown.

eastern arm of the Kimberley Arc but is close to the hinge of the arc so that the orogen has a more east-northeast trend (Fig. 13). In two samples from this area, FIA were determined from andalusite and garnet porphyroblasts (Table 1). The andalusite FIA trend  $130\text{--}135^\circ$  and are defined by inclusion trails that are truncated by the external matrix foliations. In contrast, north-northeast to northeast-trending FIA in garnet porphyroblasts from the same sample are defined by inclusion trails that are continuous with the matrix foliation. These textural relationships suggest that the east-southeast-trending andalusite FIA formed earlier than the northeast-trending garnet FIA. This timing is unusual for an andalusite-biotite-muscovite-garnet-quartz assemblage, and possible explanations include growth of pyrophyllite with later garnet growth from chlorite, or an unusual  $P\text{-}T\text{-}t$  path with an increase in  $P$  and a decrease in  $T$  after andalusite growth. Significantly, the earlier FIA set in the McClintock Range have the same trend as the earlier FIA set 200 km to the north in the Black Rock Antiform (Fig. 13).

### The younger FIA set

The younger set of FIA in both the Black Rock Antiform and McClintock Range have a narrow trend range, with an average of  $35^\circ$  (Figs. 12 and 13), similar to the regional structural trends

in these two areas. The younger timing of this FIA trend is demonstrated in the Black Rock Anticline by the fact that all but one sample preserving a  $35^\circ$ -trending FIA have a truncated core with an FIA trending  $127^\circ$ . This younger timing is supported by the fact that  $35^\circ$ -trending FIAs were derived from porphyroblasts with inclusion trails continuous with those in the matrix, whereas porphyroblasts without a  $35^\circ$ -trending rim FIA always have their inclusion trails truncated by the matrix foliation. The  $35^\circ$ -trending FIA in McClintock Range appears younger than the  $127^\circ$  FIA for similar reasons (as explained above).

### COMPARISON OF FIA TRENDS AROUND THE ARC

Comparison of FIA trends from both arms of the Kimberley Arc (Fig. 13) reveals the following important points: (1) Average FIA trends at  $127^\circ$  occur on both arms of the arc (Fig. 11), yet these arms have an angle between them of approximately  $90^\circ$ ; (2) FIA trends averaging  $127^\circ$  remain consistent across deflections in bedding trends of approximately  $45^\circ$  on either arm of the arc (Fig. 13); (3) FIA trends averaging  $127^\circ$  are unaffected by tight younger folds on the eastern arm; (4) FIA trends averaging  $127^\circ$  occur on both arms in outcrops spanning a distance of 700 km along the orogen (Figs. 11a and 11b); (5) The garnet porphyroblasts containing the bulk of these  $127^\circ$  FIAs grew around the peak of metamorphism at 1855 Ma on the western arm and 1854 Ma on the eastern arm (Page et al. 1986); and (6) Younger FIA trends averaging  $35^\circ$  are found only on the eastern arm and lie approximately parallel to its regional trend. However, a younger period of tonalite emplacement and metamorphism at 1830 Ma affected this arm (Page et al. 1986).

### COMPARISON OF FIA PLUNGES AROUND THE ARC

We measured FIA plunges in six samples with west-northwest to east-southeast trending FIA from four of the six map locations in Figure 1. We did this to test whether the FIA could have been rotated in a vertical plane striking  $127^\circ$  from the western to eastern arms of the arc. If this had happened, the FIA could just appear to not have been rotated, but the plunges should be dramatically different. The plunges for six samples with FIA trending west-northwest-east-southeast are shallow (between  $0$  and  $25^\circ$ ) to the southeast on both limbs of the arc. We also measured the FIA plunge in one sample on the eastern arm containing the younger  $35^\circ$  set and found it to be sub-horizontal (Table 1).

### INTERPRETATION

#### FIA sets on the eastern arm

The eastern arm of the Kimberley Arc underwent granitoid emplacement from 1860 to 1855 Ma and a long history of multiple deformation with the peak of metamorphism at 1854 Ma (Tyler et al. 1994; Page et al. 1995b). This was overprinted by a younger period of regional metamorphism and granite emplacement at 1830 Ma that is not present in the western arm (Page et al. 1995b; Tyler and Page 1996). Therefore, we suggest that the earlier and later FIA sets in the Black Rock Anticline correlate, respectively, with the earlier and later FIA sets in the McClintock Range and formed during these two periods

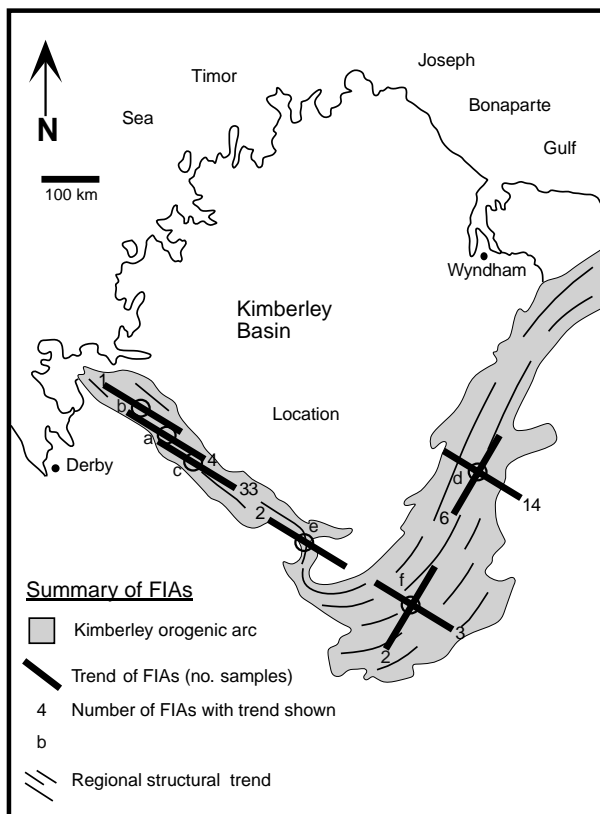


**FIGURE 13.** Map showing regional structural trend within the Kimberley Arc as well as the trends of FIA at the locations shown in Figure 1. The number of samples for which the FIA have been determined are printed alongside the trend for each location.

of metamorphism. The earlier FIA set has remained consistently oriented in spite of the dramatic re-orientation of all other earlier structures around younger folds.

### FIA sets on the western arm

The western arm of the Kimberley Arc underwent granitoid emplacement from 1865 to 1850 Ma and a long history of multiple deformation with the peak of metamorphism at 1855 Ma (Tyler et al. 1994; Page et al. 1995b). The FIAs have the same orientation in the three areas mapped in detail along this western arm as well as at Sparkes Range (Fig. 13). Although only 1, 4, and 2 FIAs were measured from areas b, c, and e, respectively (Fig. 13), 33 FIA were measured from area a. The latter group of FIAs is statistically significant and, combined with the fact that no deviation from this was found in areas a, b, c, and e, this consistent orientation strongly suggests that the FIA population in all four areas is the same and formed at the same time prior to and around the 1855 Ma peak of metamorphism. In the western arm, possibly the only expressions of the younger period of orogeny that dominates the eastern arm, are the locally developed  $D_5$  and  $D_6$  kinks with vertical axial planes striking northeast and horizontal respectively (Figs. 2a–c).

### FIA sets on both arms

Both arms of the arc preserve similar ages of granitoid emplacement, long histories of multiple deformation, and similar isotopic ages for the peak of metamorphism (see above discussion). Therefore, the  $127^\circ$ -trending FIA set on both arms and in the hinge region of the Kimberley Arc (Fig. 13) is interpreted to result from all the porphyroblasts containing this FIA trend growing during the same period of bulk shortening and accompanying metamorphism. This does not mean that all porphyroblasts grew during the same foliation-producing deformation. Deformation partitions at all scales into zones of progressive shearing and shortening, and sites for porphyroblast growth are strongly controlled by this phenomenon (Bell et al. 1986; Bell and Hayward 1991). Where orogenesis involves a succession of overprinting events during the one direction of bulk shortening, porphyroblast growth is commonly heterogeneous and records very little of the complete history of deformation that the rocks have undergone (Spiess and Bell 1996; Bell et al. 1998). Consequently, inclusion trail geometries are more commonly simple than complex (e.g., Fig. 14 in Bell and Hayward 1991) and correlation of phases of growth with individual locally developed foliations can be pointless, as the foliations themselves may be so locally developed as to not be correlatable. However, porphyroblast growth, and hence metamorphism, over the period of time that a particular direction of bulk shortening operated, can be correlated (Bell et al. 1998). We know in modern orogens that this direction can shift several times during orogenesis (Platt et al. 1989), and this provides an explanation for the regular, consecutive, and consistent pattern of shifting FIA trends in the Appalachian and Qinling Mountains where the bulk of detailed FIA work has been done (Bell et al. 1997, 1998; A. Chen, unpublished manuscript 1999; H.S. Kim, unpublished manuscript 1999).

Because the FIA plunges remain shallowly plunging around the Kimberley Arc (Table 1), the FIA cannot have been rotated

in a vertical plane during arc formation, supporting the above correlation. Because the multiple deformations that produced the eastern arm of the arc are distributed heterogeneously, both within that arm and from arm to arm, neither coaxial strain nor the rotational effects of buckling being exactly counterbalanced by the opposite rotational effects of flexural flow, can provide an explanation for these FIA remaining in the same orientation around the arc. Only a deformation mechanism involving partitioning of the progressive shearing component during each deformation entirely into cleavage seams, leaving ellipsoidal islands of unstrained porphyroblasts plus predominantly coaxially shortened strain shadows on their margins, can explain the consistent trends of these FIA around the arc (e.g., Bell and Hickey 1997).

Porphyroblasts have also grown during a younger period of bulk shortening on the eastern arm of the Kimberley Arc, but not on the western arm. FIAs trending  $35^\circ$  can be correlated among samples containing porphyroblasts with inclusion trails continuous with the matrix foliation along the eastern arm of the arc. The change in FIA trend indicates a dramatic shift in the direction of bulk shortening, which, from the geometry of the arc shown in Figure 13, has deformed and reoriented the eastern portion of the orogen to create the eastern arm. No porphyroblasts with these northeast FIA trends have been found on the western arm even though weak, local kinks with axial planes parallel to structures on the eastern arm, which overprint all northwest-southeast trending structures, may have formed at this time. These structures appear to be associated with retrogression of previously developed porphyroblastic phases, and we suggest that no porphyroblast growth took place at this time in this portion of the arc.

## DISCUSSION

### The scale of FIA consistency

The striking consistency of the first-formed FIAs around the spectacular Kimberley Arc (Fig. 13) accords well with similar data from the Vermont Appalachians. Bell et al. (1998) showed in southeast Vermont that four sets of FIA, with consistent relative timing across the region, remain consistently oriented over an area of  $125 \times 35$  km around and across multiple folds and refolds. However, the scale is much greater in the Kimberley Arc, with the FIAs retaining a consistent orientation over a distance of 700 km along the orogen. This is so even though evidence for the succession of northwest-striking foliations, preserved as inclusion trails in porphyroblasts, was completely destroyed in the matrix of the rocks in the eastern arm by the succession of intense deformations that produced the northeast structural trend of this arm. The resulting succession of northeast-striking foliations preserved in the eastern arm appears to have been produced by a dramatic shift in the direction of bulk shortening and the partitioning of this deformation almost entirely into the eastern arm.

This overprinting succession of deformations could have rotated the eastern arm through more than  $90^\circ$  to its current orientation, yet it did not affect the  $127^\circ$  trend of the first-formed FIAs. Thus intensely developed, highly partitioned deformation can completely obliterate evidence for pre-existing matrix foliations, dramatically reorientating an orogen on a large scale,

and yet leave the pre-existing FIA trends as little affected as it does on the scale of a 7 km wavelength macroscopic fold (Bell and Hickey 1997) or a  $125 \times 35$  km multiply refolded portion of an orogen with a long and complex history (Bell et al. 1998). This strongly suggests FIAs provide a very useful tool for the correlation of metamorphism around such large-scale structures.

### The significance of FIAs with regards to metamorphism

FIAs are the intersections of successive foliations preserved in porphyroblasts. Bell and Hickey (1987), Bell et al. (1997, 1998), Hickey and Bell (1999), A. Chen (unpublished manuscript 1999), and H.S. Kim (unpublished manuscript 1999) have demonstrated that FIAs remain consistently oriented over several generations of local foliation development captured by episodic, but progressive, growth of porphyroblasts during some or all of these local events, in spite of multiple folding and refolding events. They also showed that a consistent succession of shifts in FIA trend can be recorded in this manner with the relative timing revealed by changes in FIA trend from the core to rim of the porphyroblasts. This succession of FIAs appears to result from changes in the direction of horizontal bulk shortening during progressive metamorphism. Once a porphyroblast core has formed, successive foliation intersections preserved within the porphyroblast maintain consistent orientations until the direction of bulk shortening changes, provided the porphyroblast does not rotate, unlike stretching lineations and intersection axes between foliations developed in the matrix (Bell and Wang 1999). Since the technique for measurement of an FIA is completely independent of whether or not the porphyroblast rotates, the measurements allow one to test whether the porphyroblast has or has not rotated during younger ductile deformations. All FIA measurements made so far in multiply deformed schists strongly support the contention that the porphyroblasts have not rotated.

Porphyroblasts commonly record long local histories of foliation development and may enable the correlation of successively developed foliations about the one FIA trend [e.g., the staurolite porphyroblasts in Bell et al. (1997); Hickey and Bell (1999)]. However, in general they will more readily enable correlation of porphyroblast growth during a period of time which metamorphism took place about a single direction of horizontal bulk shortening. Because porphyroblasts enable one to distinguish when the direction of bulk shortening changes, they enable one to correlate the accompanying growth of porphyroblasts and hence metamorphism that takes place over a range of time. This proves extremely useful because porphyroblast growth is commonly episodic and heterogeneous from sample to sample (Bell and Hayward 1991; Spiess and Bell 1996; Stallard 1998) and, in general, these different periods of porphyroblast growth about different FIA trends cannot be distinguished and correlated by other approaches (Bell et al. 1987, 1998). Indeed, the preservation of very long histories of foliation development accompanied by metamorphism and porphyroblast growth in the Appalachians was not recognized until this type of work was started. A very significant use for FIAs is that they enable correlation of metamorphic histories between rocks that have undergone completely different *P-T-t* paths, across a large region, or across younger shear zones on which there has been large vertical displacements. For example, the metamorphic rocks either

side of the Connecticut Line between the Vermont and New Hampshire Appalachians have undergone *P-T-t* paths that differ in the pressure of peak metamorphism by 4–6 kilobars. However, four periods of porphyroblast growth (Bell et al. 1998) about a succession of differently trending FIAs is identical on either side of the Connecticut Line, enabling these different periods of growth to be correlated across this line (Kim H.S. unpublished manuscript 1999).

### Correlation of metamorphism around arcs

Virtually identical isotopic age data from both arms of the Kimberley Arc suggest that metamorphism should be correlatable from one arm to the other. However, the eastern arm also shows isotopic evidence for a younger succession of deformation and metamorphism that does not occur in the western arm. Separation of the periods of porphyroblast growth associated with each of these periods of metamorphism was not possible prior to the present study because the inclusion trails of most porphyroblasts in the eastern arm were truncated by the matrix foliation. In hindsight, these truncations provided a solution, but because deformation in young events commonly partitions intensely against porphyroblast rims, this solution was not testable (e.g., Bell and Hayward 1991). We cannot correlate porphyroblast growth at the level of successive foliations in these rocks, but we can correlate metamorphism over a period of time during which there was a consistent direction of bulk shortening generating a single FIA trend (e.g., Bell et al. 1998).

Porphyroblast growth on both arms occurred during development of a  $127^\circ$ -trending FIA set. The similar ages of granitoid emplacement (1865–1850 Ma in west vs. 1860–1855 Ma in east, Tyler et al. 1994) and similar isotopic ages for the peak of metamorphism (1855 Ma vs. 1854 Ma, Tyler et al. 1994; Page et al. 1995b) suggest that the same period of metamorphism captured this  $127^\circ$  FIA trend on both arms. This, in turn, suggests the converse, that similar FIA trends in a consistent succession may enable us to correlate the period of metamorphism over which those porphyroblasts grew, even where all affects of associated phases of deformation have been completely destroyed in the matrix (e.g., Bell et al. 1998). Thus, FIAs appear to provide a unique structural and metamorphic tool for both the preservation and correlation of events that get destroyed in the matrix. Further detailed work of this type will confirm whether or not this is the case, but the results of H.S. Kim (unpublished manuscript 1999) in the Appalachians, A. Chen (unpublished manuscript 1999) in the Qinling Orogen, China, and H. Lee (unpublished manuscript 1999) in the Ogcheon Belt, Korea, strongly support it.

The rocks on the eastern arm show a younger period of regional metamorphism and granite emplacement at 1830 Ma that is not present in the western arm (Page et al. 1995b; Tyler and Page 1996). This accords with the younger  $35^\circ$  FIA set preserved in this arm. These younger events had little impact on the western arm of the Kimberley Arc where the youngest deformations form small, locally developed kinks with northeast-striking axial planes denoted as  $S_5$  in Figure 2, and even rarer kinks with sub-horizontal axial planes denoted as  $S_6$ . The northeast strike of  $S_5$  suggests that this deformation could have resulted from the overprinting effects of successive northeast-trending deformations

that formed the eastern arm. However, no porphyroblast growth was found that accompanied these weak deformations on the western arm and there appears to have been no matrix mineral growth either, as no axial plane foliations developed.

### Significance for folding mechanism and deformation history

The lack of variation in FIA trends over large distances has important implications for the possible mechanism by which folding occurs in schist belts on all scales; it requires deformation to have occurred by progressive bulk inhomogeneous shortening (Bell and Hickey 1997; Hickey and Bell 1999). A large component of shear was involved in the formation of the Kimberley Arc, as evidenced by the trend of the western arm plus the trend of the early set of west-northwest-east-southeast FIAs preserved in the eastern arm, vs. the structural grain of the eastern arm. Yet the porphyroblasts containing the 127°-trending FIA set were not rotated as the eastern arm developed. This can be explained by a deformation history of progressive bulk inhomogeneous shortening (Bell 1981), which partitions the deformation into components of shearing and shortening. The rigid porphyroblasts do not deform and prevent an ellipsoidal island of rock in their strain shadows from undergoing significant rotational strain. In a strain field diagram of this type of deformation, portions that cannot strain internally cannot rotate (Fig. 11c in Bell and Hickey 1997). This data supports that obtained at smaller, but still macroscopic scales from Vermont (Bell and Hickey 1997; Bell et al. 1998), Connecticut (Bell et al. 1987; Hickey and Bell 1999), Massachusetts (Kim, H.S. unpublished manuscript 1999) and in the Qinling Orogen in China (Chen, A. unpublished manuscript 1999) from a range of porphyroblasts preserved in schists. All these data suggest that porphyroblasts are generally not rotated during younger ductile, single or multiple, refolding events.

### ACKNOWLEDGMENTS

We gratefully acknowledge the excellent preparation and analytical facilities provided by the School of Earth Sciences at James Cook University for conducting this type of research. Bell acknowledges funds received from the Australian Research Council. Mares acknowledges receipt of both a James Cook University Scholarship and an Overseas Postgraduate Research Scholarship. We both thank Ken Hickey for help he gave in reading and criticizing the manuscript before submission. We also thank Dave Gray, Scott Johnson, Mike Rubenach, and an anonymous referee for suggestions that they made for improving the manuscript.

### REFERENCES CITED

- Allen, R. (1985) Regional metamorphism of the Halls Creek Mobile Zone, East Kimberley, Western Australia. In K.A. Plumb, R. Allen, and S. Hancock, Eds., Conference on Tectonics and Geochemistry of Early to Middle Proterozoic fold belts. Australian Bureau of Mineral Resources Record 1985/28, 32–40.
- (1986) Relationship of thermal evolution to tectonic processes in a Proterozoic fold belt: Halls Creek Mobile Zone, East Kimberley, Western Australia. Unpublished PhD Thesis, University of Adelaide, 169 p.
- Bell, T.H. (1978) The development of slaty cleavage across the Nackara Arc of the Adelaide Geosyncline. *Tectonophysics*, 51, 171–201.
- (1981) Foliation development: the contribution, geometry and significance of progressive bulk inhomogeneous shortening. *Tectonophysics*, 75, 273–296.
- Bell, T.H. and Hayward, N. (1991) Episodic metamorphic reactions during orogenesis: The control of deformation partitioning on reaction sites and duration. *Journal of Metamorphic Geology*, 9, 619–640.
- Bell, T.H. and Hickey, K.A. (1997) Distribution of pre-folding linear movement indicators around the Spring Hill Synform, Vermont: significance for mechanism of folding in this portion of the Appalachians. *Tectonophysics*, 274, 275–294.
- Bell, T.H. and Rubenach, M.J. (1983) Sequential porphyroblast growth and crenulation cleavage development during progressive deformation. *Tectonophysics*, 92, 171–194.
- Bell, T.H. and Wang, J. (1999) Linear indicators of movement direction (mineral elongation lineations, stretching lineations and slickensides) vs. Foliation Intersection Axes in porphyroblasts (FIAs) and their relationship to directions of relative plate motion. *Earth Science Frontiers*, 6, 31–47.
- Bell, T.H., Fleming, P.D., and Rubenach, M.J. (1986) Porphyroblast nucleation, growth and dissolution in regional metamorphic rocks as a function of deformation partitioning during foliation development. *Journal of Metamorphic Geology*, 4, 37–67.
- Bell, T.H., Forde, A., and Wang, J. (1995) A new indicator of movement direction during orogenesis: measurement technique and application to the Alps. *Terra Nova*, 7, 500–508.
- Bell, T.H., Hickey, K.A., and Wang, J. (1997) Spiral and staircase inclusion trail axes within garnet and staurolite porphyroblasts from the Bolton Syncline, Connecticut: timing of growth and the effects of fold development. *Journal of Metamorphic Geology*, 15, 467–478.
- Bell, T.H., Hickey, K.A., and Upton, G.J.G. (1998) Distinguishing and correlating multiple phases of metamorphism across a multiply deformed region using the axes of spiral, staircase and sigmoidally curved inclusion trails in garnet. *Journal of Metamorphic Geology*, 16, 767–794.
- Carey, S.W. (1955) The orocline concept in geotectonics. *Proceedings of the Royal Society of Tasmania*, 89, 255–289.
- Derrick, G.M. and Playford, P.E. (1973) Lennard River, Western Australia: Western Australia Geological Survey, 1:250000 Geology Series Explanatory Notes.
- Dow, D.B. and Gemuts, I. (1969) Geology of the Kimberley Region, Western Australia: The East Kimberley, Western Australia Geology Survey, Bulletin 120.
- Gemuts, I. (1971) Metamorphic and igneous rocks of the Lamboo Complex, East Kimberley Region, Western Australia. *Australia BMR Geology and Geophysics, Bulletin 107*.
- Griffin, T.J., Tyler, I.M., and Playford, P.E. with a contribution by Lewis, J.D. (1992) Explanatory notes on the Lennard River 1:250000 Geological sheet SE/51-8 Western Australia, 3rd ed. Geological Survey of Western Australia and Department of Minerals and Energy, Record 1992/5, 85 p.
- Hickey, K. and Bell, T.H. (1999) Behaviour of rigid objects during deformation and metamorphism: a test using schists from the Bolton Synform, Connecticut. *Journal of Metamorphic Geology*, 17, 211–228.
- Mares, V.M. (1996) The structural and tectonic development of the orogens marginal to the Kimberley Province, Western Australia, and a part of the Eastern Fold belt of the Mount Isa Inlier, Queensland. Unpublished PhD Thesis, James Cook University, 220 p.
- Marshak, S. (1988) Kinematics of orocline and arc formation in thin-skinned orogens. *Tectonics*, 7, 73–86.
- Page, R.W. (1988) Geochronology of early to middle Proterozoic fold belts in northern Australia: a review. *Precambrian Research*, 40/41, 1–19.
- Page, R.W. and Sun, S.-S. (1994) Evolution of the Kimberley Region, W.A. and adjacent Proterozoic Inliers—new geochronological constraints. *Geological Society of Australia Abstracts No. 37, 12th Australian Geological Convention, Perth*, 332–333.
- Page, R.W., Hoatson, D., Sun, S.-S., and Foudoulis, C. (1995a) High-precision geochronology of Palaeoproterozoic layered mafic-ultramafic intrusions in the East Kimberley. *Australian Geological Survey Organization Research Newsletter*, 22, 7–8.
- Page, R.W., Tyler, I.M., and Blake, D.H. (1995b) Geochronology of magmatism and high-grade metamorphism, Kimberley region, W.A. (abstract) 3rd Australian Conference on Geochronology (ACOG-3); Perth, November 1995, p.25.
- Platt, J.P., Behrmann, J.H., Cunningham, P.C., Dewey, J.F., Helman, M., Parish, M., Shepley, M.G., Wallis, S., and Weston, P.J. (1989) Kinematics of the Alpine arc and the motion history of Adria. *Nature*, 337, 158–161.
- Plumb, K.A. and Gemuts, I. (1976) Precambrian Geology of the Kimberley Region, Western Australia. 25th International Geological Congress Excursion Guide 44C.
- Spiess, R. and Bell, T.H. (1996) Microstructural controls on sites of metamorphic reaction: a case study of the inter-relationship between deformation and metamorphism. *European Journal of Mineralogy*, 8, 165–186.
- Stallard, A. (1998) Episodic porphyroblast growth in the Fleur de Lys Supergroup, Newfoundland: Timing relative to the sequential development of multiple crenulation cleavages. *Journal of Metamorphic Geology*, 93, 711–728.
- Tyler, I.M. and Page, R.W. (1996) Palaeoproterozoic deformation, metamorphism and igneous intrusion in the central zone of the Lamboo Complex, Halls Creek Orogen. *Geological Society of Australia Abstracts*, 13th Australian Geological Convention, Adelaide, September, p. 450.
- Tyler, I.M., Griffin, T.J., Page, R.W., and Shaw, R.D. (1994) Are there terranes within the Lamboo Complex of the Halls Creek Orogen? *Geological Survey of Western Australia, Annual Review 1993-94*, 37–46.

MANUSCRIPT RECEIVED OCTOBER 14, 1998

MANUSCRIPT ACCEPTED JUNE 2, 1999

MANUSCRIPT HANDLED BY SCOTT JOHNSON